

Muon sites and diffusion in lithium oxide

This article has been downloaded from IOPscience. Please scroll down to see the full text article.

1998 J. Phys.: Condens. Matter 10 7975

(<http://iopscience.iop.org/0953-8984/10/36/008>)

View [the table of contents for this issue](#), or go to the [journal homepage](#) for more

Download details:

IP Address: 171.66.16.210

The article was downloaded on 14/05/2010 at 17:16

Please note that [terms and conditions apply](#).

Muon sites and diffusion in lithium oxide

J S Lord, S P Cottrell and W G Williams

ISIS Facility, Rutherford Appleton Laboratory, Central Laboratory of the Research Councils,
Chilton, Didcot, Oxon OX11 0QX, UK

Received 13 May 1998, in final form 6 July 1998

Abstract. Muon spin relaxation (μ SR) measurements have been performed on the alkali metal oxides Li_2O and Na_2O in order to model the behaviour of hydrogen impurities in these materials. Lithium oxide has been suggested as a suitable blanket material for fusion reactions, hence the need to understand the location and dynamics of T^+ ions in the crystalline lattice. This oxide becomes a fast ion conductor at high temperatures ($T \sim 1000$ K) and our experiments also provide information on the Li^+ ion dynamics.

Muon implantation into these oxides at low temperatures ($T \sim 10$ K) creates mainly neutral muonium (the analogue of the hydrogen atom) with a smaller fraction ($\sim 20\%$) of positive muons μ^+ at interstitial sites closely associated with O^{2-} ions. At higher temperatures ($T > 100$ K) the proportion of μ^+ formed increases, and there is an increased tendency for trapping at substitutional lattice sites. A sharp decrease in relaxation rate was observed in Li_2O at temperatures above 250 K and from this temperature dependence we calculate the activation energy for muon hopping relative to the Li^+ ions, which are also mobile, to be approximately 90 meV.

1. Introduction

Lithium oxide, Li_2O , has important technological applications as a leading candidate for a blanket material in future fusion reactors [1]. The blanket converts energetic neutrons into usable heat and breeds the tritium required to sustain the D–T fusion reaction using the reaction ${}^6\text{Li} + n \rightarrow {}^3\text{H} + \alpha$. Its advantages as a blanket to surround the plasma vessel stem from its high Li atom density, high melting point ($T_m = 1705$ K), low tritium solubility, high thermal conductivity and fast tritium release.

It is of importance to ascertain the charge states, lattice sites and the diffusion of tritium in this material at a microscopic level, but this has been extremely challenging experimentally. Nuclear magnetic resonance [2] and neutron scattering [3] have been used to measure lithium diffusion at high temperatures (~ 1000 K) where the material becomes a fast-ion conductor, and the assumption has been made that the dynamics of the T^+ ions and Li^+ ions are correlated [4]. Direct experimental observations of the T^+ behaviour are, however, limited to bulk diffusion measurements, although the subject has attracted considerable theoretical interest. The *ab initio* electronic structure calculations of Shah *et al* [5] predicted the energies and likely location of tritium as a substitutional defect associated with a Li^+ vacancy (T_{Li}), and of tritium as an interstitial defect separated from the Li vacancy ($\text{T}_i^+ + \text{V}_{\text{Li}}^-$). In both cases the tritium is found to be bonded to an oxide ion to form OT^- with an O–T spacing of 0.99 Å. A further conclusion of this work was that the T^+ and Li^+ dynamics are not necessarily correlated (although the activation energies are similar) and that the most likely diffusion path for interstitial T^+ is hopping between nearest-neighbour oxide ions.

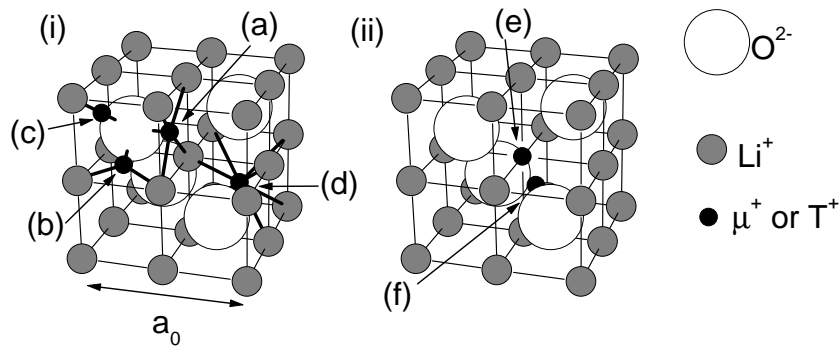


Figure 1. (i) Structure of Li_2O and possible interstitial muon/tritium sites. (a), (b), (c) are at 0.99 \AA from an oxide ion in the (100), (110) and (111) directions, (d) is the 'empty cube centre' site. Lines show the nearest-neighbour ions. (ii) Substitutional sites in Li_2O . (e) is on the vacant Li lattice site, (f) is at 0.99 \AA from one of the four neighbouring oxide ions, pointing towards the vacant Li site.

The antifluorite crystal structure of Li_2O may be considered as a simple cubic array of Li^+ ions of spacing $a_0/2 = 2.304 \text{ \AA}$ (at 293 K), with the O^{2-} ions occupying alternate cube centres; see figure 1. The structure and sites of the tritium centres produced following neutron capture are not known, although the triton ion is expected to recoil from the lithium vacancy produced with it. In this paper we have used muon spin relaxation (μSR), where the muon acts as a light isotope of tritium ($m_\mu/m_T = 1/27$), as a microscopic probe to provide information on the trapping sites and diffusion of hydrogen-like defects in the Li_2O crystal lattice. Similar studies have been performed in other proton conductors, such as perovskites [6]. The implantation of surface positive muons (energy $\sim 4 \text{ MeV}$) can be expected to closely mimic the behaviour of the recoil T^+ ions (energy $\sim 2.7 \text{ MeV}$) following the neutron capture by ${}^6\text{Li}$, and μSR provides us with an experimental technique to determine the local structural environment and dynamics of μ^+ . We note that the subsequent diffusion of μ^+ will be faster than for T^+ because of the lower mass.

As an adjunct to our principal objective in studying hydrogen-like centres in lithium oxide, we also describe corresponding μSR measurements for sodium oxide which has a much lower ionic conductivity. These experiments enabled us to confirm our interpretation of the (nuclear) magnetic interactions and dynamics in Li_2O . For static muon and nuclear moments the observed muon linewidths can be compared with the nuclear dipolar linewidths calculated using the Van Vleck function with second moment given by

$$\Delta^2 = (2/3)I(I+1)\hbar^2 \sum_{j=1}^N \gamma_j^2/r_j^6$$

where γ_j and r_j are the gyromagnetic ratios and distances from the muon of the nuclei (${}^6\text{Li}$, ${}^7\text{Li}$, ${}^{23}\text{Na}$) contributing to the linewidth, and I is the nuclear spin quantum number. Table 1 shows calculated values for $\sigma = \gamma_\mu \Delta$ (μs^{-1}) for a range of muon sites in the Li_2O and Na_2O fluorite structures.

If the nuclei have spin $I > 1/2$ and are in an electric field gradient (EFG), the presence of a quadrupole interaction may modify the linewidth. If the quadrupole splitting is greater than the dipolar interaction the nuclear spin is quantized along the EFG axis. For an EFG directed towards the muon's point charge and nuclear spin $I = 3/2$ the linewidth is reduced by a factor $(4/5)^{0.5} = 0.894$. A simple point charge calculation for the interstitial site (a) would predict a quadrupole interaction $eqQ = 0.65 \text{ MHz}$ in Li_2O and 0.87 MHz in

Table 1. Calculated dipolar muon linewidths $\sigma = \gamma_\mu \Delta$ (μs^{-1}) in Li_2O and Na_2O . Note that the relaxed lattices are based on the *ab initio* calculations of Shah *et al* [5].

Type	Site	Host lattice	Linewidths	
			Li_2O	Na_2O
Interstitial (μ_i^+)	(a) 0.99 Å from O^{2-} in the (100) direction	Fixed	0.6875	0.2682
		Relaxed	0.5144	
	Rapid hopping between the 6 (a) sites around the same oxide ion	Fixed	0.4113	0.1868
	(b) 0.99 Å from O^{2-} in the (110) direction	Relaxed	0.5283	
	(c) 0.99 Å from O^{2-} in the (111) direction	Relaxed	0.5149	
	(d) Empty cube centre	Fixed	0.5286	0.2135
Substitutional (μ_{Li}^0)	(e) Centred vacant Li^+ site	Fixed	0.3371	0.1362
	(f) 0.99 Å from O^{2-} in the (111) direction towards the vacancy	Fixed	0.415	
		Relaxed	0.4222	0.1767
	Rapid hopping between the 4 (f) sites around the Li^+ vacancy	Fixed	0.311	

Na_2O , implying that the quadrupole corrections should be applied. However, ^7Li NMR measurements in doped Li_2O [2] show a quadrupole splitting of only ~ 0.04 MHz for Li nuclei near defect sites so some screening of the electric fields must be taking place. These defect sites may be Li nearest-neighbour vacancies (V_{Li}^-), calculated $eqQ = 0.23$ MHz, or F^- substituting for O^{2-} (F_O^+), 0.35 MHz. The substitutional sites (e) and (f) have zero net charge so should give much lower (if any) quadrupole effects.

A muon hopping rapidly between a small number of sites (as distinct from a freely diffusing muon) still shows a Gaussian lineshape. Such rapid hopping (or reorientation of OH^-) is observed by quasi-elastic neutron scattering in other oxides [7]. The field seen by the muon is the vector average of the local fields at each site visited. The Van Vleck second moment can be calculated by randomly choosing orientations of near-neighbour spins and calculating the local field, then averaging over all possible spin configurations using a Monte Carlo technique. Table 1 includes the results for two possible cases. Since the sites have some nearest neighbours in common, the linewidth for a set of N sites is reduced from that of a single site by a factor smaller than $N^{0.5}$.

2. Muon spin relaxation

The positive muon, μ^+ , is an unstable elementary particle (mean lifetime ~ 2.2 μs) with a mass m_μ approximately one-ninth of the proton mass m_p , a spin $\frac{1}{2}$ and a magnetic moment $8.89 \mu_N$. Muon beams are produced by the collinear decay of positive pions $\pi^+ \rightarrow \mu^+ + \nu_\mu$ (mean lifetime ~ 26 ns) and are 100% polarized in the direction opposite to the μ^+ momentum. The polarization property (which can be exploited experimentally because one of the μ^+ decay products, the positron e^+ , is detected following preferential emission in the polarization direction) is responsible for the high sensitivity of muon techniques, and only a small number of stopped muons (10^2 – 10^3) are present in the investigated samples at any particular time.

The muon may be stopped in virtually any material and its spin interactions monitored to provide information on the static and fluctuating magnetic fields from neighbouring nuclear and atomic moments. In the experiments to be described the magnetic interactions are only between the muon and ^6Li and ^7Li nuclear moments in Li_2O and the ^{23}Na nuclear moments

in Na₂O. The magnetic moments and natural abundances (in parentheses) for the magnetic nuclei are: ⁶Li (7.42%) 0.8219 μ_N; ⁷Li (92.58%) 3.257 μ_N; ²³Na (100%) 2.216 μ_N. Muon techniques include spin rotation, spin relaxation and spin resonance, collectively known as μSR, although in this paper we are concerned only with muon spin relaxation in zero magnetic field (ZF-μSR).

Following implantation into the sample, the initial polarization vector of the muon spin ensemble either precesses in, or is relaxed by, the magnetic fields from local nuclear dipoles. Our experiments were carried out in zero applied magnetic field in which the time dependence of this depolarization over 10–20 μs after implantation is determined by measuring the anisotropy of the emitted positrons as a function of time. The experiments were performed on the ARGUS and EMU muon spectrometers at the ISIS pulsed muon source, where the accelerator pulse provides the time zero (*t*₀) trigger.

The experimental set-up consists of forward (F) and backward (B) scintillation counters relative to the beam direction, and the measured asymmetry spectrum, *A*(*t*), is defined by

$$A(t) = [I_F(t) - \alpha I_B(t)] / [I_F(t) + \alpha I_B(t)]$$

where the *I*'s represent time differential positron counts in the F and B detectors and α is a correction factor to account for inequalities in the F and B detector assembly efficiencies. *A*(*t*) is proportional to the time-dependent muon polarization, with $A(t) = A_0 P(t)$, where *A*₀ is the maximum measurable asymmetry which is instrument dependent with a typical magnitude of ~0.25. The two experimental observables of interest are *A*(*t*), which is related to the relaxation function representing the muon/nuclear spin interactions, and *A*₀, the initial asymmetry, which can reveal rapid initial depolarization as occurs, for example, in zero-field experiments if the positive muon captures an electron to form neutral muonium. Experimental studies by Kudo and Okuno [8] have shown that the tritium charge state in n-irradiated Li₂O is T⁺, although our μSR results show that muon thermalization into both μ⁺ and neutral Mu (muonium) states takes place at temperatures less than 300 K.

3. Experimental results

3.1. Lithium oxide

Figure 2(b) shows the initial asymmetry *A*₀ observed in polycrystalline Li₂O at temperatures between 20 K and 330 K. The results indicate that a large fraction (~80%) of neutral muonium is formed at the lowest temperatures and that this fraction decreases only very gradually, reaching ~70% at the highest temperatures. The most probable positions for muonium in the fluorite structure of Li₂O are at interstitial sites at the empty cube centres. The remaining fraction of muons, whose relaxation can be observed, is expected to be bonded to O²⁻ ions to form the OMu⁻ ion. However, as the O²⁻ ion has no unpaired electrons and no nuclear moment it has no effect on the muon's spin.

The relaxation functions *A*(*t*) measured over the same temperature have been modelled using a stretched exponential function $P(t) = \exp(-(\lambda t)^\beta)$ and the relaxation rates λ derived from these fits are shown in figure 2(a).

Below 80 K the μ⁺ observed relaxation function is essentially Gaussian ($\beta = 2$) showing that the muons are static at interstitial sites. The linewidth $\sigma = \lambda = \gamma_\mu \Delta \approx 0.406(7) \mu\text{s}^{-1}$ is consistent with a local structure where the muon is bonded to a O²⁻ ion with an O-μ distance of 0.99 Å, but freely rotating around it much more rapidly than the observed relaxation rate, as in table 1. This agrees with the results obtained by Shah *et al* [5] where the energy barrier for rotation is only 0.05 eV, which is probably less than the zero-point

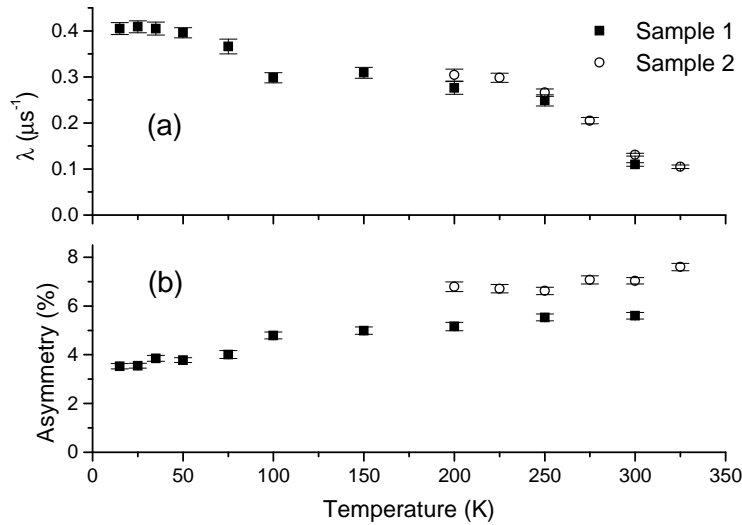


Figure 2. (a) Relaxation rate λ and (b) initial asymmetry A_0 for Li_2O as a function of temperature.

energy of the muon. However, we cannot discount the possibility that the muon is bonded to one of the oxide ions next to a Li vacancy, site (f) in table 1.

Between 80 and 100 K the μ^+ relaxation function becomes more Lorentzian ($\beta \rightarrow 1$) and the relaxation rate falls to about $0.3 \mu\text{s}^{-1}$. This is indicative of the onset of muon dynamics where either the diffusion is between interstitial sites or the muons become trapped at Li^+ vacancy sites (but where the neighbouring Li^+ ions are static). Between 100 and 200 K the relaxation rate remains constant but, however, it is still Lorentzian in form. The linewidth (when fitted to a Gaussian relaxation function) corresponds to a substitutional site where the muon is either centred on the Li vacancy lattice site or rapidly hopping between the equivalent sites at 0.99 \AA from the four neighbouring O^{2-} ions, as predicted to be the stable site for T^+ by Shah *et al* [5]. The apparent Lorentzian nature of the relaxation function $P(t)$ can be explained by a small Lorentzian contribution from the muonium fraction, with a rapid relaxation rate of the order of $1\text{--}5 \mu\text{s}^{-1}$. This is supported by measurements in an applied magnetic field transverse to the initial muon polarization, which shows a lower initial asymmetry.

The relaxation rate decreases sharply above 250 K and in this regime the Li^+ ions and the muons both occupy substitutional sites and are highly mobile; this is the classical motional narrowing condition in magnetic resonance. This observation is in agreement with ^7Li nuclear magnetic resonance (NMR) data [2] which shows the linewidth starting to decrease at around 300 K, followed by a large decrease at 450–600 K when all the ^7Li nuclei are involved in the motion within the measuring time. It is of interest to note that both μSR and NMR have the sensitivity to observe ionic mobilities in the precursor phase to the ‘fast-ion’ conduction phase in Li_2O . Neutron diffraction, in contrast, requires Li^+ Frenkel defect concentrations of a few per cent to provide a useful change in the diffraction signal, and this only occurs at temperatures in excess of 1200 K [9], which is well into the ‘fast-ion’ conduction regime.

The decrease in relaxation rate which sets in at around 250 K can be used to calculate the activation energy for muon hopping relative to the Li^+ ions. The relaxation curves were fitted with the zero-field Abragam function [10, 11]

$$P(t) = \exp[-2(\sigma\tau)^2\{\exp(-t/\tau) - 1 + t/\tau\}]$$

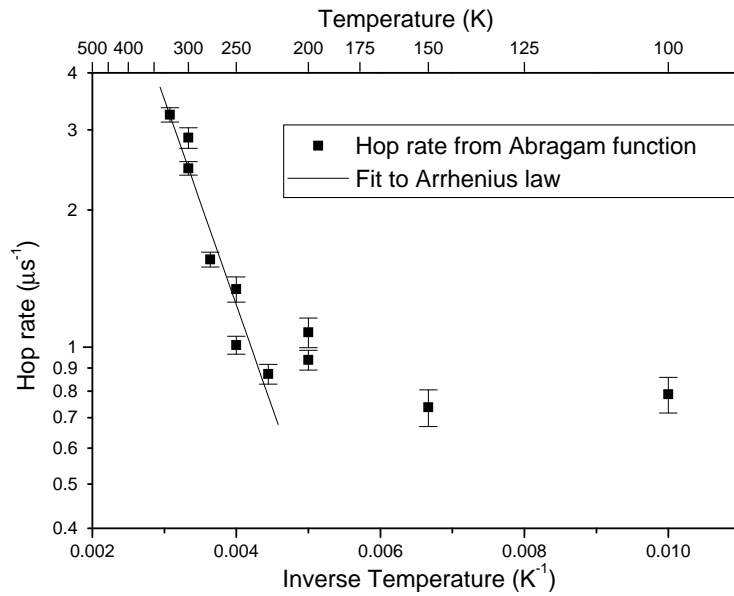


Figure 3. Hopping rate for muons in Li_2O giving the activation energy.

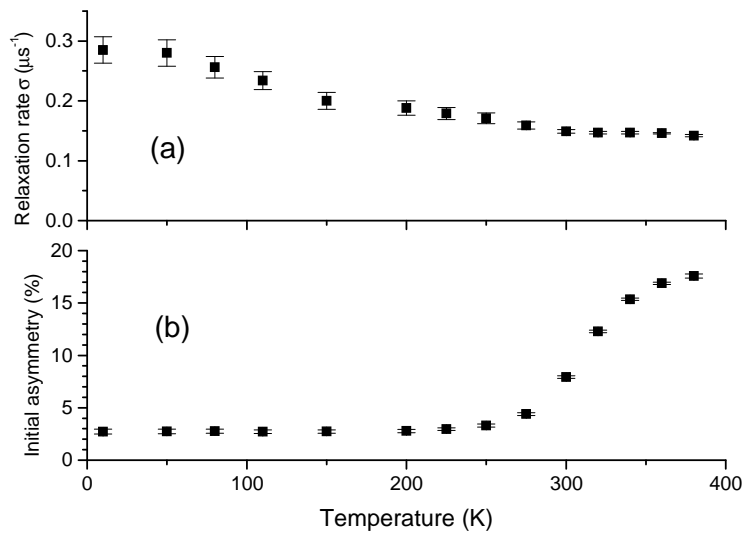


Figure 4. (a) Relaxation rate σ and (b) initial asymmetry A_0 for Na_2O as a function of temperature.

which models the relaxation of a spin hopping between equivalent sites at a rate $(1/\tau)$. The static linewidth σ was set from the low-temperature data. Plotting $\log(\text{hop rate})$ against inverse temperature and fitting a straight line gives an activation energy of about 90 meV; see figure 3. Setting σ by fitting the data around 100 K with $\tau = 0$ gives an activation energy of ~ 190 meV.

Measurements of T^+ diffusion give an activation energy from 0.5 eV (T dissolved) to 1.0 eV (irradiated) [1]. *Ab initio* calculations give 0.45 eV for hopping between interstitial sites or 1.75 eV for hopping between substitutional sites (Li^+ vacancies) [5].

^7Li NMR relaxation rate and linewidth measurements have been made on pure Li_2O [2]. Motional narrowing gives T_2 proportional to $1/\tau$ in the case of $\tau \ll T_2$, so fitting to the Arrhenius behaviour $\tau(T) = \tau_0 \exp(E_a/kT)$ gives an apparent activation energy of about 0.4 eV for the motion of the Li^+ ions. The hop rate of a host Li^+ ion is related both to the mobility of the defect or vacancy and to the number of such vacancies, both of which increase with temperature. In a pure sample where all the defects are created by thermal activation this is likely to lead to an overestimate of E_a . However, data for 1% LiF doped Li_2O gives a very similar activation energy, which suggests that the nominally pure sample has enough impurities to give extrinsic behaviour at the temperatures studied.

The onset of the NMR linewidth change is around 300 K, although the main effect of motional narrowing is seen between 450 and 600 K, where the mean residence time for a Li^+ ion is comparable to T_2 for the static lattice ($\approx 50 \mu\text{s}$). With less than 1% of defects the hop rate for the vacancy will be over 100 times faster than that of an individual Li^+ ion, and would probably be comparable to the muon linewidth at around 300 K. It is therefore likely that the increase in the muon hop rate around 300 K is related to the onset of Li^+ ion motion.

3.2. Sodium oxide

Similar μSR experiments were also carried out on Na_2O which has the same antiferroite crystal structure as Li_2O , but with a larger lattice dimension where the cubic array of Na^+ ions have a spacing $a_0/2 = 2.775 \text{ \AA}$ (at 293 K). This material does not become a fast ion conductor at elevated temperatures, but was studied because it provides another magnetic nucleus to help confirm our interpretation of the magnetic interactions and dynamics in these oxides. A large muonium fraction $\sim 80\%$ was also observed in Na_2O at low temperatures. In contrast to Li_2O , this fraction decreased dramatically at approximately 300 K, as indicated by the sharp increase in the initial asymmetry A_0 in figure 4(b) for the diamagnetic μ^+ fraction. The muonium fraction also had a much lower relaxation rate than in Li_2O , obscuring the first $\approx 1 \mu\text{s}$ of the diamagnetic spectrum.

Figure 4(a) shows the relaxation rates derived from the relaxation functions measured for Na_2O . The fits to a Gaussian lineshape are shown; however, a Lorentzian lineshape was also used and sometimes gave a better fit to the data. A more general lineshape, such as the stretched exponential or Abragam function, could not be fitted because of the initial rapid relaxation of the muonium fraction.

At low temperatures the μ^+ lineshape is Gaussian showing that the muons are static. The linewidth $\sigma = 0.282(16) \mu\text{s}^{-1}$ is consistent with an interstitial μ^+ location at approximately 1.0 Å from an O^{2-} ion, oriented in the (100) direction: site (a) in figure 1. Assuming that none of the ions move from their lattice sites, the linewidth would be $\sigma = 0.2682 \mu\text{s}^{-1}$, as in table 1.

Between 80 and 300 K the lineshape becomes Lorentzian with a relaxation rate falling with increasing temperature, corresponding to muons diffusing between interstitial sites. The change of linewidth with temperature is slow, giving an activation energy of 15 meV. This may be expected if the muon is able to fit between the much larger Na^+ and O^{2-} ions.

Above 300 K the lineshape returns to Gaussian with a lower linewidth $\sigma = 0.147(2) \mu\text{s}^{-1}$, due to muons trapped at Na^+ vacancies. The calculated relaxation rate for such a substitutional site (table 1) is $\sigma = 0.1362 \mu\text{s}^{-1}$ for a muon centred at a Na^+ vacancy and $\sigma = 0.1767 \mu\text{s}^{-1}$ for the off-centre O^{2-} bonded site as predicted for Li_2O . The rate of diffusion of Na^+ ions must be very low (less than $0.05 \mu\text{s}^{-1}$) for the static muon lineshape to be observed up to 400 K. Unlike Li_2O , Na_2O is not an ionic conductor.

4. Conclusions

The predominant muon state observed following positive muon implantation into Li_2O and Na_2O is neutral muonium, Mu , and is suggestive that the existence of tritium atoms in n-irradiated Li_2O cannot be dismissed, particularly at ambient temperatures and below. This contrasts with the findings of Kudo and Okuno [8] for almost exclusive triton formation, but is qualitatively reasonable because inclusion of a neutral atom into the ionic lattice requires a lower energy. Interstitial hydrogen atoms take up the empty cube centre sites in fluorite structures such as CaF_2 [12], and by analogy the most probable Mu sites in these antiferroite structures are also at the centres of the empty cubes in the crystalline lattice. However, the muon measurements observe the charge state within the first $\sim 20 \mu\text{s}$ after implantation while neutron irradiation and the subsequent observation of tritium content may take many hours.

At low temperatures ($< 20 \text{ K}$) the thermalized positive muons remain static and closely bonded to O^{2-} ions in both oxides. At higher temperatures ($20 \text{ K} < T < 250 \text{ K}$) the positive muons start to diffuse, and there is an increased tendency for trapping at vacant Li^+ (Na^+) substitutional sites; indeed, in Na_2O a static μ^+ Gaussian relaxation behaviour was observed characterized by a width corresponding to the ^{23}Na nuclear moment environment at this site. The temperature increase also increases the fraction of muons thermalizing in the μ^+ state. This was more evident in Na_2O which has the larger lattice constant and where positive ion repulsion is smaller.

Above 250 K the μ^+ relaxation rate in Li_2O decreases rapidly due to fast Li^+ diffusion and the increased availability of substitutional vacancies. This observation is consistent with NMR observations, and supports the hypothesis that the μ^+ (T^+) and Li^+ dynamics are correlated at high temperatures in this fast-ion conductor. The high temperature μ^+ relaxation rate observed in Na_2O remained constant up to 380 K , which is indicative of very slow Na^+ ion mobility.

Acknowledgment

We acknowledge Dr S Hull for his loan of a Li_2O sample and for useful discussions.

References

- [1] Johnson C E and Hollenberg G W 1984 *J. Nucl. Mater.* **122/123** 871
- [2] Xie Z H, Smith M E, Strange J H and Jaeger C 1995 *J. Phys.: Condens. Matter* **7** 2479
- [3] Hutchings M T, Clausen K, Dickens M H, Hayes W, Kjems J K, Schnabel P G and Smith C 1984 *J. Phys. C: Solid State Phys.* **17** 3903
- [4] Ohno H, Konishi S, Nagasaki T, Kurasawa T, Katsuta H and Watanabe H 1985 *J. Nucl. Mater.* **133/134** 181
- [5] Shah R, De Vita A and Payne M C 1995 *J. Phys.: Condens. Matter* **7** 6981
- [6] Hempelmann R, Soetratmo M, Hartmann O and Wäppling R 1998 *Solid State Ionics* **107** 269
- [7] Matzke Th, Stimming U, Karmonik Ch, Soetratmo M, Hempelmann R and Güthoff F 1996 *Solid State Ionics* **86-66** 621
- [8] Kudo H and Okuno K 1986 *J. Nucl. Mater.* **138** 31
- [9] Farley T W D, Hayes W, Hull S, Hutchings M T and Vrtis M 1991 *J. Phys.: Condens. Matter* **3** 4761
- [10] Abragam A 1961 *Principles of Nuclear Magnetism* (Oxford: Oxford University Press)
- [11] Keren A 1994 *Phys. Rev. B* **50** 10039
- [12] Sligar S G and Blum H 1971 *Phys. Rev. B* **3** 3587